



# Exosome-Mediated Communication in Thyroid Cancer: Implications for Prognosis and Therapeutic Targets

Yiwei Wang<sup>1,2,7</sup> · Qiang Li<sup>3</sup> · Xinrui Yang<sup>2</sup> · Hanyu Guo<sup>1</sup> · Tian Ren<sup>4</sup> · Tianchi Zhang<sup>5</sup> · Pantea Ghadakpour<sup>6</sup> · Fu Ren<sup>1,7</sup>

Received: 17 September 2023 / Accepted: 8 May 2024

© The Author(s), under exclusive licence to Springer Science+Business Media, LLC, part of Springer Nature 2024

## Abstract

Thyroid cancer (THCA) is one of the most common malignancies of the endocrine system. Exosomes have significant value in performing molecular treatments, evaluating the diagnosis and determining tumor prognosis. Thus, the identification of exosome-related genes could be valuable for the diagnosis and potential treatment of THCA. In this study, we examined a set of exosome-related differentially expressed genes (DEGs) (BIRC5, POSTN, TGFBR1, DUSP1, BID, and FGFR2) by taking the intersection between the DEGs of the TCGA-THCA and GeneCards datasets. Gene Ontology (GO) and Kyoto Encyclopedia of Genes and Genomes (KEGG) analyses of the exosome-related DEGs indicated that these genes were involved in certain biological functions and pathways. Protein–protein interaction (PPI), mRNA–miRNA, and mRNA-TF interaction networks were constructed using the 6 exosome-related DEGs as hub genes. Furthermore, we analyzed the correlation between the 6 exosome-related DEGs and immune infiltration. The Genomics of Drug Sensitivity in Cancer (GDSC), the Cancer Cell Line Encyclopedia (CCLE), and the CellMiner database were used to elucidate the relationship between the exosome-related DEGs and drug sensitivity. In addition, we verified that both POSTN and BID were upregulated in papillary thyroid cancer (PTC) patients and that their expression was correlated with cancer progression. The POSTN and BID protein expression levels were further examined in THCA cell lines. These findings provide insights into exosome-related clinical trials and drug development.

**Keywords** Thyroid cancer · Papillary thyroid cancer · Exosome · BID · POSTN

---

Yiwei Wang and Qiang Li contributed equally to this work.

Extended author information available on the last page of the article

## Introduction

Thyroid cancer (THCA) stands as the most prevalent endocrine malignancy, and it has become the fastest rising cancer worldwide in terms of its incidence. Previous findings have shown that THCA is the 5th most common malignancy after breast cancer, lung cancer, colorectal cancer, and cervical cancer in females. In China, THCA incidences have surged over recent decades. Treatments for THCA include resection and radioactive iodine therapy; however, there is no effective treatment for refractory THCA. More recently, biomarker-driven therapies were speculated to be promising treatments for a subset of THCA (Fan et al. 2019; Pozdeyev et al. 2018). Hence, it is urgent to better understand the underlying mechanisms of THCA progression, which might enhance the diagnosis and effective treatments of this disease.

Extracellular vesicles (EVs) include exosomes, microvesicles, apoptotic bodies, and viral particles (Jiang et al. 2017; Nolte-'t Hoen et al. 2016; Xie et al. 2019). In particular, exosomes have attracted much attention in recent years. Exosomes are extracellular vesicles 30–150 nm in diameter that are derived from the fusion of multivesicular endosomes, generated by endosomal membranes and released into the extracellular space (Gan et al. 2020; Villarroya-Beltri et al. 2016; Xie et al. 2019). Biologically, exosomes are an important source of proteins that mediate cell-to-cell communication and modulate the tumor microenvironment (Allenson et al. 2017; Lang et al. 2018). A number of studies have reported that exosomes have significant value in terms of performing molecular treatments, evaluating the diagnosis of THCA and determining the prognosis of THCA (1988; Capriglione et al. 2022; Maggisano et al. 2022; Xin et al. 2022; Zou et al. 2020). Consequently, exosomes have emerged as important factors in elucidating the underlying disease mechanisms and identifying diagnostic and therapeutic strategies for THCA.

Advanced molecular and bioinformatics technologies have led to the confirmation of many novel biomarkers in THCA (Agarwal et al. 2021). In addition, in THCA, genetic genomic analyses were performed on the TCGA cohort, with a focus on differential genes, oncogenic drivers, pathological classification, molecular subtypes, and so on (Cancer Genome Atlas Research 2014; Ganly et al. 2018; Ibrahimasic et al. 2017; Yoo et al. 2019). Because exosomes can intercellularly communicate with and regulate the tumor microenvironment (TME), they can be used to diagnose, predict, and treat cancer (Qiu et al. 2021; Wu et al. 2019). Understanding the clinical and molecular roles of exosome-based cancer therapy is crucial for cancer treatment and prognosis.

The purpose of our study was to identify and evaluate the clinical significance of exosome-related genes in THCA patients and explore the mechanisms of exosome-related genes in the progression of THCA. First, the DEGs and exosome-related genes were intersected to obtain exosome-related DEGs through the TCGA and GeneCards databases. The exosome-related DEGs were further analyzed by enrichment of Gene Ontology/The Kyoto Encyclopedia of Genes (GO/KEGG) analyses. In addition, we constructed a protein–protein interaction

(PPI) network and mRNA–miRNA and mRNA–transcription factor (TF) interaction networks of the exosome-related DEGs. The expression of exosome-related DEGs was verified via Gene Expression Omnibus (GEO) data. Furthermore, immune infiltration correlation and drug sensitivity analyses were performed. We next validated that the DEGs were related to the clinical tissues of thyroid cancer. Moreover, the expression and molecular correlation analysis of BID and POSTN were evaluated through tissue microarrays (TMAs) of our clinical tissue samples. We also examined relative RNA and protein expression levels in thyroid cancer cell lines.

## Materials and Methods

### Data Download

The expression profiles of THCA patients were downloaded from the GEO (<http://www.ncbi.nlm.nih.gov/geo/>) database (Barrett et al. 2013) using the R packages GEOquery (Davis and Meltzer 2007), and the GSE3467 (He et al. 2005) and GSE3678 datasets. The GSE3467 dataset was obtained from *Homo sapiens*; the data type was mRNA, and the data platform used was the GPL570 [HG-U133A\_2] Affymetrix Human Genome U133A 2.0 Array. There were 18 samples in total, including 9 THCA samples (group: THCA) and 9 control samples (group: normal). The GSE3678 dataset was obtained from *Homo sapiens*; the data type was mRNA; and the data platform used was the GPL570 [HG-U133A\_2] Affymetrix Human Genome U133A 2.0 Array. There were 14 samples in total, including 7 THCA samples (group: THCA) and 7 samples from a control group (group: normal).

In addition, we downloaded the count sequencing data of the TCGA-THCA dataset from the TCGA (<https://portal.gdc.cancer.gov/>) (Tomczak et al. 2015) through the TCGA bio links package (Colaprico et al. 2016). The data were normalized to fragments per kilobase per million (FPKM) values. The TCGA-THCA dataset included a total of 568 samples, including 510 THCA samples (group: THCA) and 58 control samples (group: normal). The corresponding clinical information was downloaded from the UCSC Xena database (<http://genome.ucsc.edu>), and the expression profile data of all the samples were included in subsequent analyses.

The GeneCards database (Safran et al. 2010) (<https://www.genecards.org/>) provides comprehensive information on human genes. To obtain exosome-related genes, we used the word “exosome” as the search key to obtain the exosome-related genes that were identified in the literature (Lin et al. 2022), and the 121 exosome-related genes (Table S1) were intersected to obtain 63 exosome-related genes (Table S2).

### Exosome-Related Differentially Expressed Genes

We first used the limma package (Ritchie et al. 2015) to normalize the gene expression profile data of 568 samples in the TCGA-THCA dataset and constructed a PCA

plot to show the effect before and after normalization. Differential analysis was performed to obtain all DEGs with a  $\log_2FC > 1$  and a  $p$  value  $< 0.05$ . The DEGs and exosome-related genes were intersected to obtain exosome-related DEGs. The expression profile data of exosome-related DEGs in the TCGA-THCA dataset were subsequently extracted, and the ComplexHeatmap package was used to construct a heatmap to display the gene expression.

### GO and KEGG Analysis

GO analysis (Gene Ontology 2015) is a standard method for large-scale functional enrichment studies and includes biological process (BP), molecular function (MF), and cellular component (CC) analyses. The KEGG (Kanehisa and Goto 2000) and Genome databases are widely used for storing information about genomes, biological pathways, diseases, and drugs. The clusterProfiler package (Yu et al. 2012) was used to perform GO and KEGG annotation analysis on exosome-related DEGs. The entry screening criteria  $p$  value  $< 0.05$  and FDR value ( $q$  value)  $< 0.05$  were considered statistically significant, and the Benjamini–Hochberg (BH) correction was used.

### PPI Network

A PPI network is composed of proteins that interact with each other. The STRING database searches for interactions between known and predicted proteins. In this study, we used the STRING database to construct a PPI network (minimum required interaction score) from the screened exosome-related DEGs (medium confidence [0.150]), and we visualized the PPI network model using Cytoscape (Shannon et al. 2003) (version 3.9.1).

### mRNA–miRNA and mRNA-TF Interaction Networks

The Starbase database (Li et al. 2014) searches for microRNA targets through high-throughput CLIP-Seq experimental data and degradome experimental data to provide a variety of visual interfaces for exploring microRNA targets. The database contains a wealth of data for miRNA–ncRNA, miRNA–mRNA, miRNA–RNA, and RNA–RNA networks. The miRDB database (Chen and Wang 2020) was used for miRNA target gene prediction and functional annotation. We used the Starbase database and miRDB database to predict miRNAs that interact with exosome-related DEGs and then evaluated the intersection of the two database results via Cytoscape software to construct an mRNA–miRNA interaction network.

The CHIPBase database (version 2.0) (<https://rna.sysu.edu.cn/chipbase/>) (Zhou et al. 2017) identified thousands of binding motif matrices and their binding sites from ChIP-seq data of DNA-binding proteins and predicted millions of transcriptional regulatory relationships between TFs and genes. The TF target database (<http://bioinfo.life.hust.edu.cn/hTFtarget>) (Zhang et al. 2020) is a comprehensive database of human TFs and their target regulation. We searched for TFs bound to

exosome-related DEGs through the CHIPBase database (version 2.0) and hTFtarget database and visualized them using Cytoscape software.

### **Verification of the Expression of Exosome-Related Differentially Expressed Genes**

We used the limma package to normalize the GSE3467 and GSE3678 datasets. We used THCA samples (group: THCA) and control samples (group: normal) as groups to construct exosome-related differential expression group comparisons of gene expression differences among the different groups (group: high and group: low) in the GSE3467 dataset, the GSE3678 dataset and the TCGA-THCA dataset. These comparisons verified the exosome-related differences found in the TCGA-THCA dataset of exosome-related DEGs.

### **Immune Infiltration**

Single sample gene set enrichment analysis (ssGSEA) is an extension of GSEA that allows one to define an enrichment score for the pairing of a sample and a gene set. The infiltration abundance of immune cells in the TCGA-THCA cohort was calculated using the ssGSEA algorithm (Newman et al. 2015). Next, we analyzed the correlation between the infiltration abundance of immune cells and exosome-related DEG expression.

### **Drug Sensitivity Analysis of the Exosome-Related DEGs**

The Genomics of Drug Sensitivity in Cancer (GDSC, [www.cancerRxgene.org](http://www.cancerRxgene.org)) (Yang et al. 2013) is the largest public database for determining the drug sensitivity and drug response molecular markers of cancer cells. The CCLE database (<https://portals.broadinstitute.org/ccle>) (Barretina et al. 2012) consists of 24 drugs spanning 947 cancer cell lines and was used to predict the correlation of specific gene expression with drug sensitivity. The CellMiner database (<https://discover.nci.nih.gov/cellminer/>) (Reinhold et al. 2012) is a public database that contains genomic and pharmacological information for conducting analysis. The CellMiner database stores the molecular spectrum data of NCI-60 cells and other cancer cell types and is currently the most widely used database for cancer drug testing. Based on the expression of key genes and the drug data in the GDSC, CCLE, and CellMiner databases, we carried out drug sensitivity analysis on the exosome-related DEGs and displayed the results.

### **Clinical Samples and IHC**

A total of 135 PTC tissue samples were collected from the Affiliated Central Hospital of Shenyang Medical College from 2012 to 2018. The samples were classified as TNM I, II, III, or IV based on the World Health Organization (WHO) guidelines. This study was approved by the Ethical Committee of the First Affiliated Hospital of Shenyang Medical College. Paraffin-embedded tissue samples were used to

construct the tissue microarray (TMA) using a manual tissue microarray (Quick-ray, UniTMA, Seoul, South Korea). IHC was performed on the TMA, and the intensity scoring standards were described in our previous publication (Wang et al. 2020). The primary antibodies used were rabbit anti-BID polyclonal antibody (1:150; 10,988-1-AP; PTG, China) and POSTN polyclonal antibody (1:150; 19899-1-AP; PTG, China). An UltraSensitive TM SP (Mouse/Rabbit) IHC Kit (KIT-9710, Maixin, Shenzhen, China) was used to label the tissue.

## q-PCR

Total RNA was isolated using an RNA Easy Fast Kit (TianGen) and quantified. Then, the RNA was reverse transcribed into cDNA using an RT reagent kit (TaKaRa) according to the manufacturer's protocol. Real-time PCR was performed using a CFX Real-Time PCR Detection System (Bio-Rad), and the results were analyzed with CFX Manager Software (Bio-Rad). Briefly, the reaction mixtures were incubated at 95 °C for 15 min; 40 cycles of 95 °C for 5 s; and 60 °C for 35 s; and a melt step. The relative target gene expression was determined with the comparative delta-delta CT method ( $2^{-\Delta\Delta C_t}$ ). The primer sequences for the human BIRC5 gene were 5'CACCGCATCTCTACATTCA3' (sense) and 5'CAAGTCTGGCTCGTTC3' (antisense); for the human POSTN gene, 5'GACGGTGACAGTATAACAGT3' (sense) and 5'GGCAGAATCAGGAATTAGGA3' (antisense); for the human TGFBR1 gene, 5'TGAAGCCTTGAGAGTAATGG3' (sense) and 5'TGACTGAGTTGCCATTAATGT3' (antisense); for the human DUSP1 gene, 5'TGTGAAATCTGCCCTTT3' (sense) and 5'GATGTCTGCCTTGTGGTT3' (antisense); for the human BID gene, 5'AGAAGAAGTTGCTGTGAAGA3' (sense) and 5'TTGTATCCGTGGCTGAATC3' (antisense); for the human FGFR2 gene, 5'AGACTACCTGGAGATAGCC3' (sense) and 5'CTTCTTGTCGTGTTCTTC3' (antisense); and for the human housekeeping gene  $\alpha$ -TUBULIN the primers were 5'TGACCTGATGTATGCCAAG3' (sense) and 5'TTAGTATTCCCTCTCCTTCTTCC3' (antisense).

## Cell Culture and Western Blot

The human thyroid carcinoma cell lines TPC1 and K1 were kindly provided by Dr. Wei Sun (The First Affiliated Hospital of China Medical University), who purchased them from Shanghai HonSun Biological Technology Co., Ltd. BHT101 and B-CPAP were purchased from the Cell Bank of the Shanghai Chinese Academy of Sciences. The normal thyroid follicular epithelium cell line (nthy-ori3-1) was obtained from the American Type Culture Collection (ATCC), and the cells were cultured in RPMI 1640 medium (Gibco, NY, USA) with 10% fetal bovine serum (FBS; HyClone, UT, USA). TPC1 cells were cultured in Dulbecco's modified Eagle's medium (DMEM; Gibco, NY, USA) supplemented with 10% FBS. K1 cells were cultured in 50% DMEM supplemented with 25% Ham's F12 medium and 25% MCDB105 supplemented with 2 mM glutamine and 10% FBS. BHT101 cells were cultured in 6 ml of Glutamax medium (Gibco, NY, USA) and 125 ml of FBS per 500 ml of DMEM. B-CPAP cells were cultured in RPMI 1640 medium (87 ml), 10 ml of FBS, 1 ml

of NEAA (Invitrogen, USA), 1 ml of Glut Amax (Invitrogen, USA), and 1 ml of sodium and pyruvate 100 mM solution (Invitrogen, USA). All the cells were cultured under a 5% CO<sub>2</sub> atmosphere at 37 °C. The cells were lysed in RIPA buffer, and the total protein concentration was quantified with a BCA kit (P0010, Beyotime, Shanghai, China). Samples (20 µg protein) were subjected to SDS–PAGE and further transferred to polyvinylidene fluoride (PVDF) membranes. The PVDF membranes were cut following incubation with primary (BID and POSTN, 1:1000; PTG; Tubulin, 1:5000; Abcam) and secondary antibodies (anti-rabbit IgG and anti-mouse IgG, 1:5000; Cell Signaling Technology). The immunoblots were visualized using an enhanced chemiluminescence (ECL) Western blot detection system.

## Statistical Analysis

All the data were processed and analyzed with R software (version 4.2.1). For the comparison of two groups of continuous variables, the statistical significance of normally distributed variables was estimated by the independent Student *t* test, and the differences between nonnormally distributed variables were analyzed by the Mann–Whitney *U* test (ice, Wilcoxon rank sum test). The chi-square test or Fisher's exact test was used to compare and analyze the statistical significance of differences between two groups of categorical variables. All *p* values were two-sided, and *p* < 0.05 was considered to indicate statistical significance.

## Results

### Differential Analysis of Exosome-Related Genes

We first used the limma package to standardize the gene expression profile data of 568 samples in the TCGA-THCA dataset and constructed a principal component analysis (PCA) plot to evaluate the effects of normalization (Fig. 1A, B). A comparison of the PCA plots revealed that the differences between the standardized data samples slightly decreased. The results are as follows: The TCGA-THCA dataset included a total of 1478 DEGs that satisfied  $|\log\text{FC}| > 1$  and *p* < 0.05; at this threshold, upregulated genes ( $\log\text{FC} > 1$  and *p* < 0.05) were associated with 817, and downregulated genes ( $\log\text{FC} < 0$  and *p* < 0.05) were associated with 661. A volcano plot was drawn according to the different analysis results of this dataset (Fig. 1C). Next, we constructed a Venn diagram by examining the intersection of the DEGs and exosome-related genes (Fig. 2D). We obtained 6 exosome-related DEGs (BIRC5, POSTN, TGFBR1, DUSP1, BID and FGFR2), extracted the TCGA-THCA dataset from the exosome-related DEG expression profile data using the ComplexHeatmap package to construct heatmaps (Fig. 1E) and evaluate gene expression. Through the heatmap, we found that the expression levels of the DEGs in the different groups (THCA and normal) were significantly different.

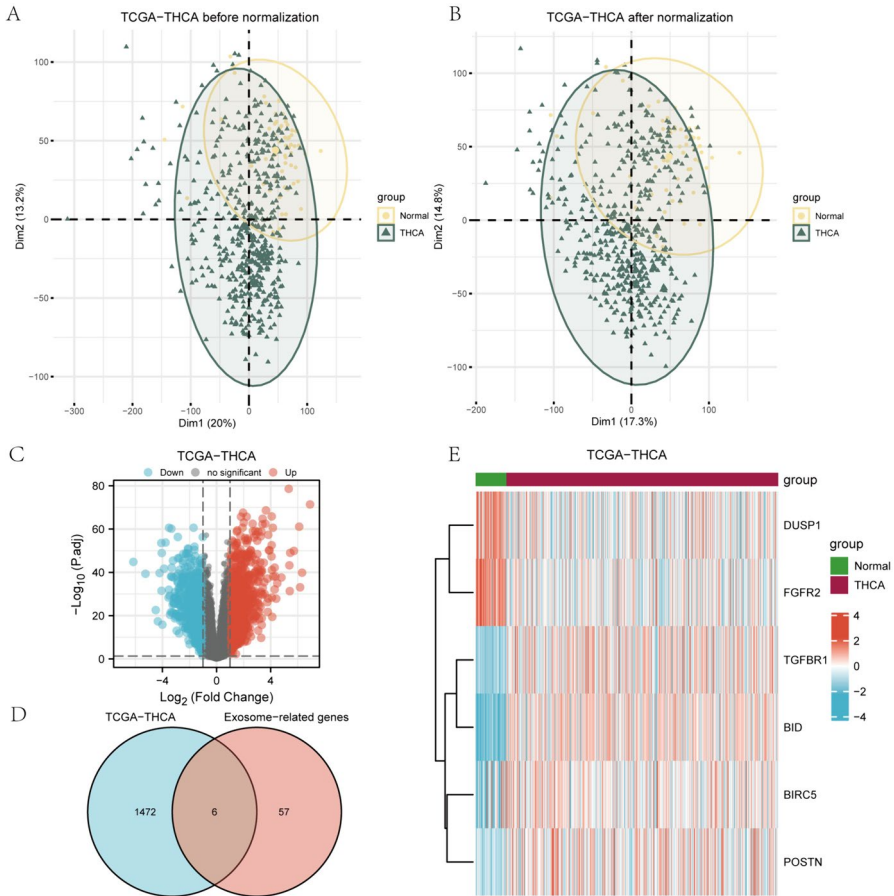


**Fig. 1** Volcano plot heatmap of differentially expressed genes in the PCA map before and after TCGA-THCA normalization and a Venn diagram of exosome-related genes. **A** PCA plot of the TCGA-THCA dataset before normalization. **B** PCA plot after normalization of the TCGA-THCA dataset. **C** Volcano plot of the differences between the THCA group and the normal group in the TCGA-THCA dataset. **D** Venn diagram of the intersection of DEGs and exosome-related genes in the TCGA-THCA dataset. **E** Heatmap of the expression profile data of exosome-related DEGs in the TCGA-THCA dataset

### GO Functional Analysis and KEGG Pathway Enrichment Analysis

We applied these 6 exosome-related DEGs (BIRC5, POSTN, TGFBR1, DUSP1, BID, and FGFR2) to perform GO and KEGG enrichment analyses. The exosome-related DEGs were upregulated mainly in the BP (cellular response to transforming growth factor beta stimulus, response to transforming growth factor beta, ventricular septum morphogenesis), CC (collagen-containing extracellular matrix, excitatory synapse, and spindle microtubule) and MF (growth factor binding, transmembrane receptor protein kinase activity and heparin binding). Moreover, genes associated with hepatitis B, apoptosis-multiple species, the MAPK

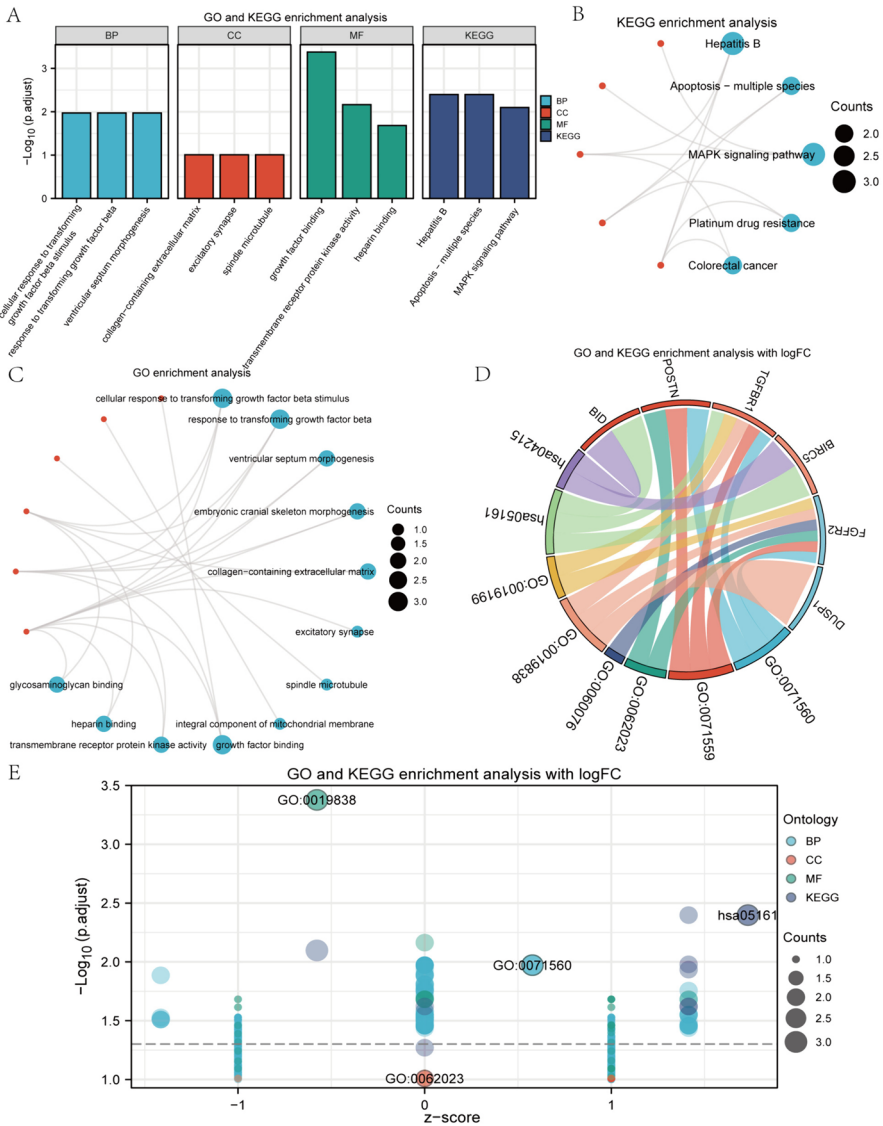


**Fig. 2** GO functional analysis and KEGG pathway enrichment analysis of exosome-related DEGs in THCA. **A** Histogram of GO and KEGG analyses of exosome-related DEGs. **B**, **C** Circular network of KEGG and GO analysis results of exosome-related DEGs. **D** Chord plot of the combined logFC results of the GO and KEGG analyses of exosome-related DEGs. **E** Bubble plot of combined logFC results from GO and KEGG analyses of exosome-related DEGs

signaling pathway, platinum resistance and the colorectal cancer pathway were also upregulated. The results of the GO and KEGG analyses were visualized by histograms (Fig. 2A) (For specific enrichment KEGG results, Table 1).

**Table 1** The enrichment results of GO and KEGG analysis

Ontology	Description	Gene ratio	BgRatio	p value	p.adjust	q value
BP	Cellular response to transforming growth factor beta stimulus	3/6	249/18670	4.55e-05	0.011	0.004
BP	Response to transforming growth factor beta	3/6	255/18670	4.89e-05	0.011	0.004
BP	Ventricular septum morphogenesis	2/6	44/18670	8.09e-05	0.011	0.004
BP	Embryonic cranial skeleton morphogenesis	2/6	45/18670	8.47e-05	0.011	0.004
BP	Ventricular cardiac muscle tissue morphogenesis	2/6	48/18670	9.65e-05	0.011	0.004
CC	Collagen-containing extracellular matrix	2/6	406/19717	0.006	0.098	0.059
CC	Excitatory synapse	1/6	50/19717	0.015	0.098	0.059
CC	Spindle microtubule	1/6	59/19717	0.018	0.098	0.059
CC	Integral component of mitochondrial membrane	1/6	73/19717	0.022	0.098	0.059
CC	Intrinsic component of mitochondrial membrane	1/6	74/19717	0.022	0.098	0.059
MF	Growth factor binding	3/6	137/17697	8.92e-06	4.19e-04	1.60e-04
MF	Transmembrane receptor protein kinase activity	2/6	79/17697	2.92e-04	0.007	0.003
MF	Heparin binding	2/6	169/17697	0.001	0.021	0.008
MF	Glycosaminoglycan binding	2/6	229/17697	0.002	0.021	0.008
MF	Sulfur compound binding	2/6	250/17697	0.003	0.021	0.008
KEGG	Hepatitis B	3/5	162/8076	7.69e-05	0.004	0.003
KEGG	Apoptosis – multiple species	2/5	32/8076	1.51e-04	0.004	0.003
KEGG	MAPK signaling pathway	3/5	294/8076	4.52e-04	0.008	0.006
KEGG	Platinum drug resistance	2/5	73/8076	7.92e-04	0.010	0.008
KEGG	Colorectal cancer	2/5	86/8076	0.001	0.012	0.009

GO, gene ontology; BP, biological process; MF, molecular function; CC, cellular component; KEGG, Kyoto encyclopedia of genes and genomes



## Construction of the PPI Network and the mRNA-TF and mRNA–miRNA Interaction Networks

Using the STRING database to perform protein–protein interaction analysis of the 6 exosome-related DEGs (BIRC5, POSTN, TGFBR1, DUSP1, BID, and FGFR2), we constructed a protein–protein interaction (PPI) network of exosome-related DEGs via Cytoscape software (Fig. 3A). The specific PPI network relationships are shown in Table S3. We used the CHIPBase database (version 2.0) and the hTFtarget database to identify TFs, and we subsequently evaluated the intersection of the two databases to construct an mRNA-TF interaction network through the use of Cytoscape software for visualization (Fig. 3B). The specific mRNA-TF interactions are shown in Table S4. We predicted miRNAs that interact with these 6 exosome-related DEGs (BIRC5, POSTN, TGFBR1, DUSP1, BID, and FGFR2) using mRNA–miRNA data from the Starbase database and the miRDB database. The intersection of the two databases was subsequently used to construct the mRNA–miRNA interaction network via Cytoscape software for visualization (Fig. 3C). The specific mRNA–miRNA interactions are shown in Table S5.

### Exosome-Related DEGs in THCA

We first used the limma package to standardize the GSE3467 and GSE3678 datasets. Six exosomes were obtained from thyroid carcinoma (THCA) samples (group: THCA) and control samples (group: normal) as exosome-related differentially expressed genes (exosome-related DEGs) in the GSE3467 (Fig. 4A) and GSE3678 (Fig. 4B) datasets.

To verify the expression of exosome-related DEGs (BIRC5, POSTN, TGFBR1, DUSP1, BID, and FGFR2), we first analyzed the expression of the exosome-related DEGs in THCA samples in comparison with that in normal tissues in the GSE3467 dataset. The results showed that BIRC5, TGFBR1, and BID were upregulated in THCA samples. However, FGFR2 and DUSP1 were downregulated in THCA tissues compared to normal tissues, but the difference in the expression of the POSTN gene was not statistically significant (Fig. 4A). Moreover, based on the GSE3678 data, the expression levels of POSTN, TGFBR1, BID and BIRC5P were upregulated in THCA tissues, but the expression levels of DUSP1 and FGFR2 appeared to be downregulated in THCA tissues compared with normal tissues (Fig. 4B). In addition, we further analyzed the mRNA expression of exosome-related DEGs in THCA patients from the TCGA dataset. The results showed that the BIRC5, POSTN, TGFBR1, and BID expression levels were greater in the THCA group than in the normal group, while DUSP1 and FGFR2 were expressed at lower levels in the THCA group (Fig. 4C). Taken together, these data confirmed that BIRC5, TGFBR1, and BID were upregulated in THCA and that DUSP1 and FGFR2 were downregulated.

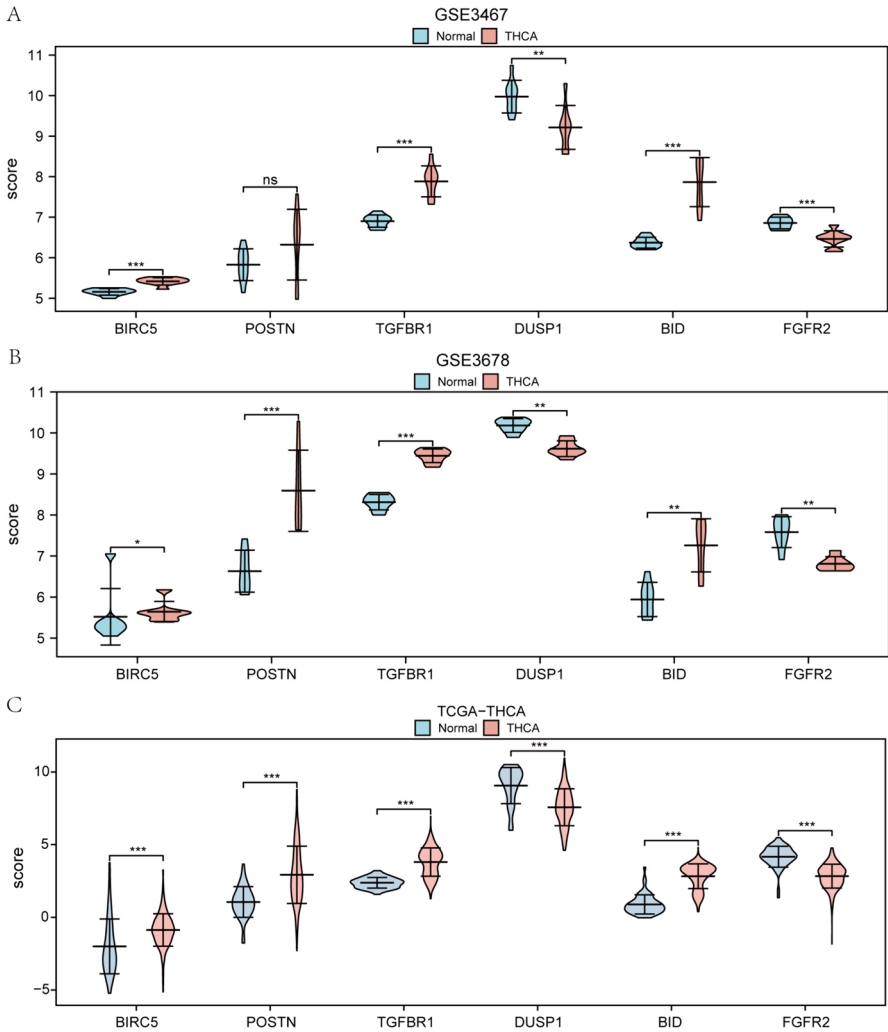


**Fig. 4** Group comparison of exosome-related DEGs in the dataset. **A** Group comparison diagram of exosome-related DEGs in the GSE3467 dataset. **B** Group comparison to the GSE3678 dataset. **C** Comparison of TCGA-THCA cohort data. ns  $p \geq 0.05$ , \*  $p < 0.05$ , \*\*  $p < 0.01$  and \*\*\*  $p < 0.001$

### Immune Infiltration Correlation Analysis of Exosome-Related DEGs

First, infiltration of 28 immune cell types in the THCA cohort was determined using the ssGSEA method, and a total of 20 immune cells (activated dendritic cells, CD56bright natural killer cells, CD56dim natural killer cells, central memory CD4 T cells, central memory CD8 T cells, effector memory CD4 T cells, eosinophils, gamma delta T cells, immature B cells, immature dendritic cells, macrophages, MDSCs, memory B cells, natural killer cells, neutrophils, plasmacytoid dendritic cells, regulatory T cells, T follicular helper cells, type 1 T helper cells, and Type

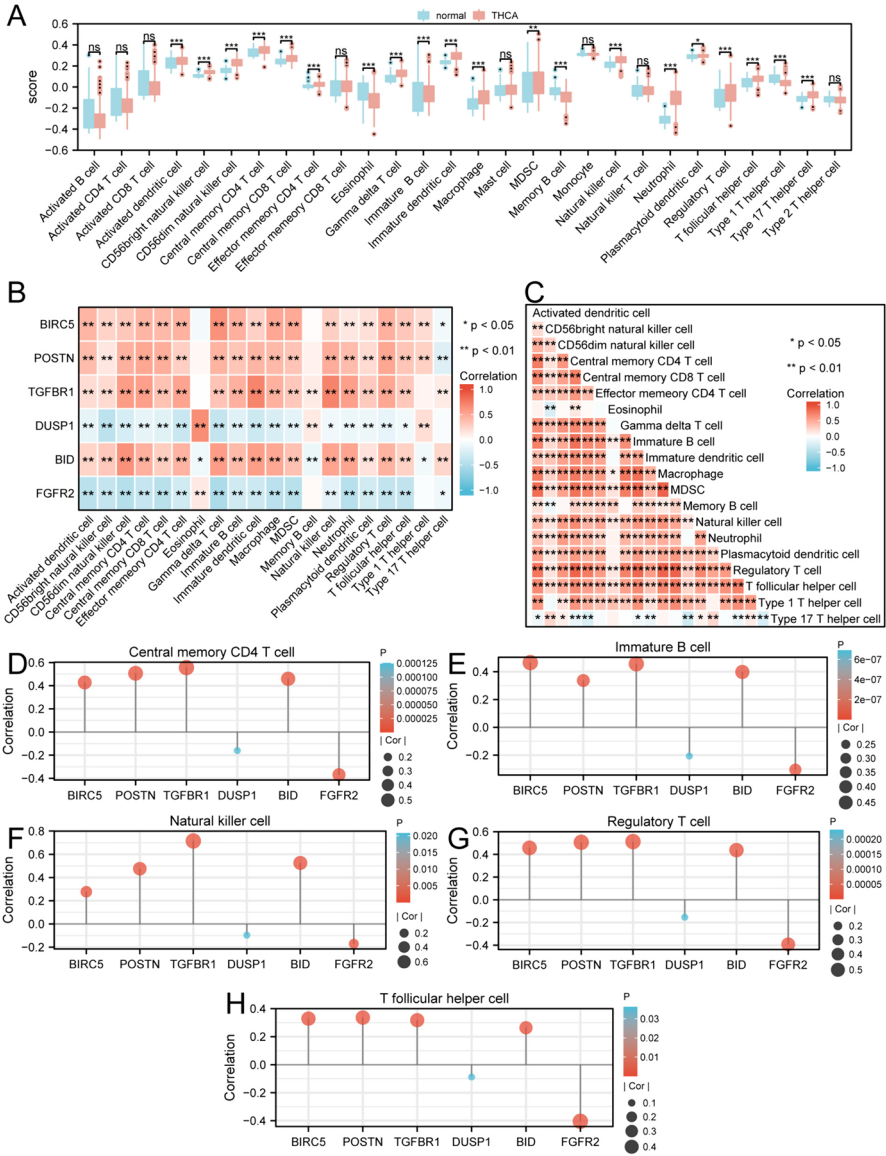


**Fig. 5** Immune infiltration analysis of exosome-related DEGs. **A** Comparison of immune cells between the normal and tumor groups in the TCGA-THCA cohort. **B** The correlation between exosome-related DEGs and immune cell infiltration. **C** The correlation heatmap for the immune cells. Correlations between exosome-related DEGs and **D** central memory CD4 T cells, **E** immature B cells, **F** natural killer cells, **G** regulatory T cells, and **H** T follicular helper cells. ns  $p > 0.05$ ; \*  $p < 0.05$ ; \*\*  $p < 0.01$ ; \*\*\*  $p < 0.001$

17 T helper cells) were significantly correlated ( $p < 0.05$ ) under the grouping of THCA and normal (Fig. 5A). Subsequently, the relationship between the exosome-related DEGs (BIRC5, POSTN, TGFBR1, DUSP1, BID, FGFR2) and immune cell infiltration was visualized using a heatmap, and BID was associated with the most (20 types) immune cells (Fig. 5B). We demonstrated the correlations among the 20 immune cells through a heatmap (Fig. 5C). Central memory CD4 T cells, immature B cells, natural killer cells, regulatory T cells, and T follicular helper cells were highly correlated with the other 20 immune cells in the dataset. Therefore, we investigated the relationship between the above 5 cell lines and exosome-related DEGs (Fig. 5D–H).

### Drug Sensitivity Analysis of Exosome-Related DEGs

Changes in the cancer genome strongly affect the clinical response to treatment and, in many cases, are effective biomarkers of drug treatment response. For drug

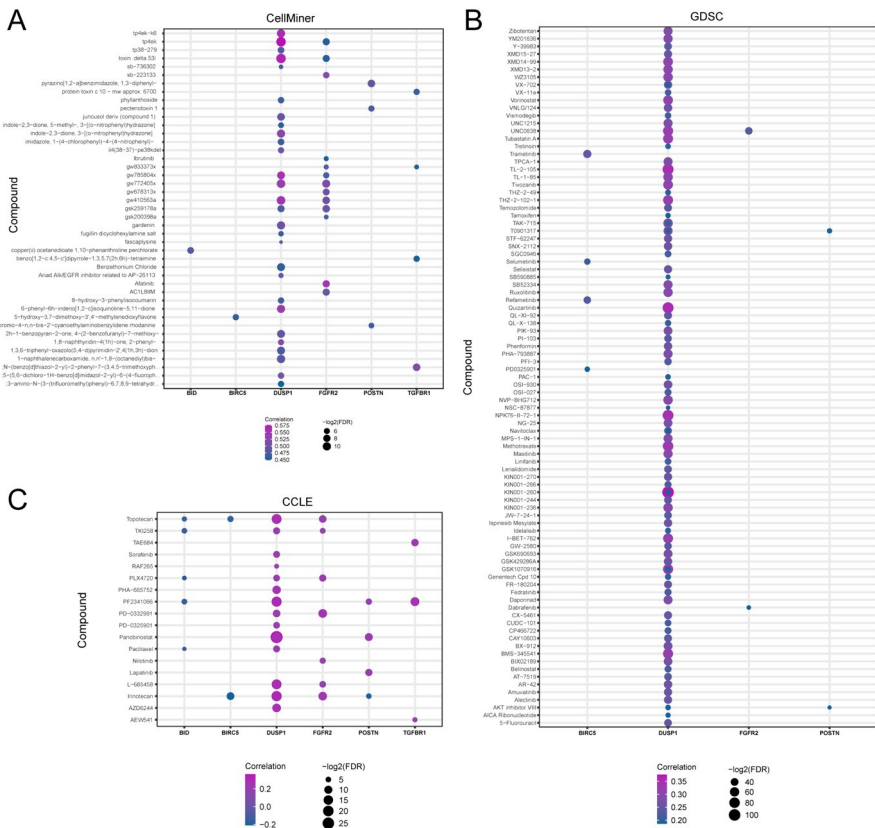


**Fig. 6** Correlation analysis between drug sensitivities and exosome-related DEGs. Overview of drug sensitivity in patients in the **A** CellMiner dataset, **B** GDSC dataset, and **C** CCLE dataset in this study

sensitivity data, the Genomics of Drug Sensitivity in Cancer (GDSC), Cancer Cell Line Encyclopedia (CCLE), and CellMiner databases were used to reveal the relationship between exosome-related DEGs and drug profiles. We predicted that the expression of exosome-related DEGs was correlated with anticancer drug sensitivity by the IC50 value and visualized the results in the CellMiner database (Fig. 6A), GDSC database (Fig. 6B), and CCLE database (Fig. 6C). The results showed that DUSP1 interacted with most of the drug molecules in the three databases; however, no drugs were found to interact with TGFBR1 or BID in the GDSC database.

### Expression Levels of Exosome-Related DEGs in PTC Tissues

To further examine the association of exosome-related DEGs, we first validated the mRNA expression of the 6 exosome-related DEGs (BIRC5, POSTN, TGFBR1, DUSP1, BID and FGFR2; Fig. 7A–F) in 15 PTC tissues and paired adjacent tissues by q-PCR and observed that POSTN and BID were upregulated in PTC tissues and that DUSP1 and FGFR2 were downregulated; however, neither BIRC5 nor TGFBR1 was significantly upregulated.

### POSTN and BID Expression Levels were Correlated with Clinicopathological Outcomes in PTC Patients

We selected the genes (POSTN and BID) upregulated in tumors for further experiments. IHC was used to evaluate the protein expression of POSTN and BID in PTC (Fig. 8A, B), and the correlation between clinicopathological features and the relative expression of the proteins was analyzed. As shown in Table 2, BID expression was significantly correlated with age ( $p < 0.001$ ), tumor size ( $p < 0.001$ ), lymph

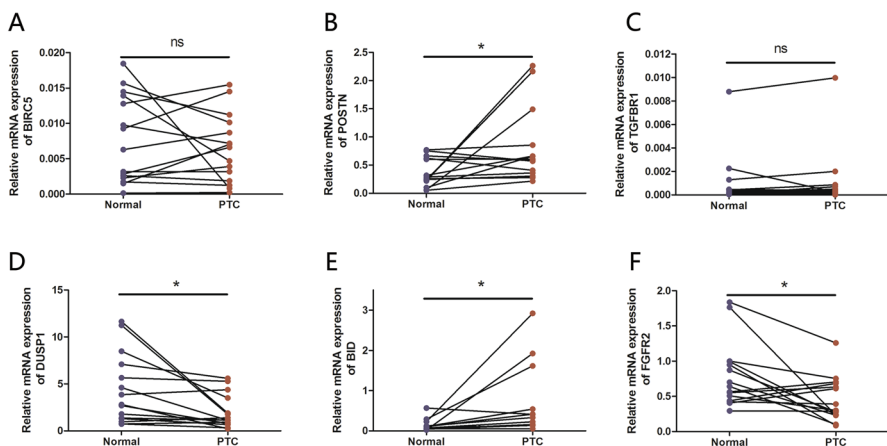


**Fig. 7** q-PCR results of exosome-related DEGs in PTC tissues. The mRNA expression levels of **A** BIRC5, **B** POSTN, **C** TGFBR1, **D** DUSP1, **E** BID, and **F** FGFR2 in PTC patient tissues. ns  $p > 0.05$ ; \* $p < 0.05$

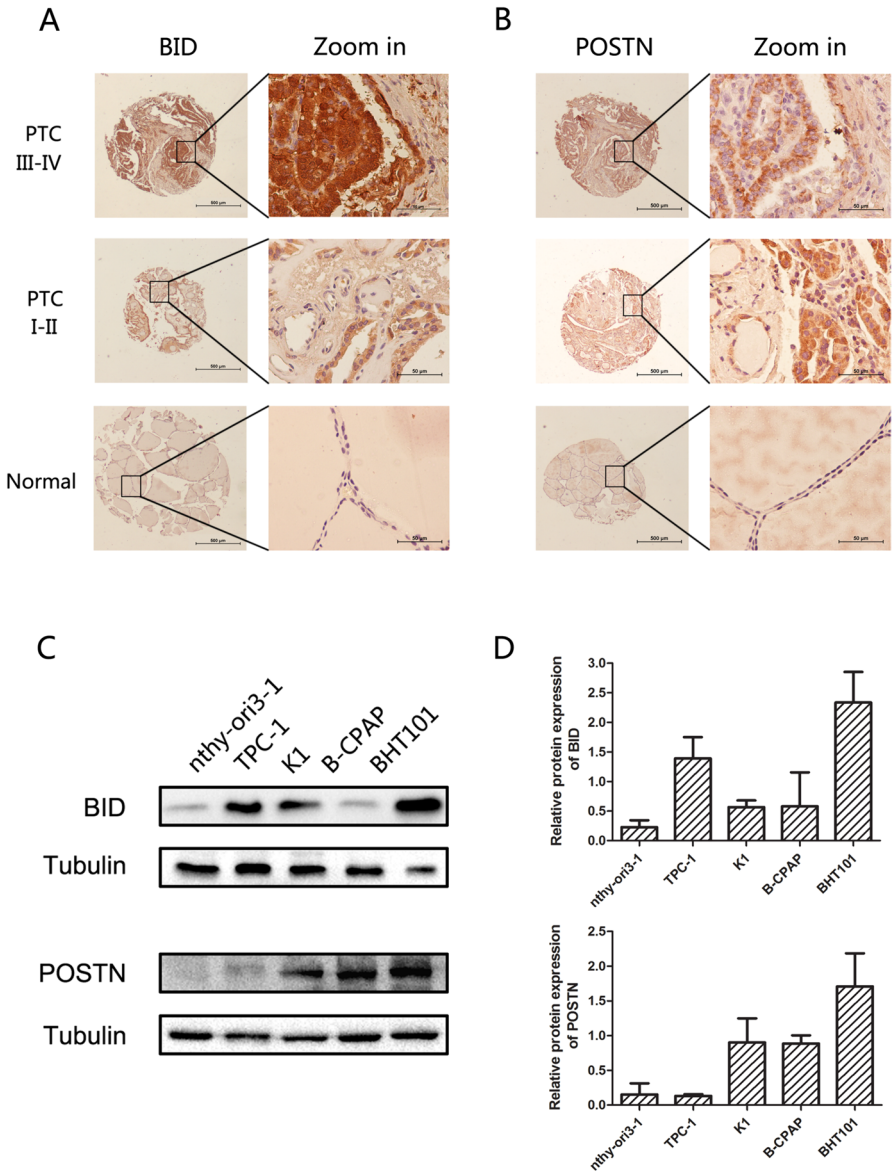


**Fig. 8** Expression of BID and POSTN in PTC cells. The expression of BID (**A**) and POSTN (**B**) in PTC and normal tissues determined by IHC (scale bar = 500  $\mu$ m; zoom in section = 50  $\mu$ m). **C**, **D** Western blot images and analyses of BID and POSTN expression

node metastasis ( $p=0.001$ ), extrathyroidal extension ( $p<0.001$ ) and TNM stage ( $p<0.001$ ). There were no significant differences in sex ( $p=0.262$ ). POSTN expression was associated with tumor size ( $p=0.012$ ), lymph node metastasis ( $p<0.001$ ), and TNM stage ( $p=0.019$ ). However, age ( $p=0.781$ ), sex ( $p=0.185$ ) and

**Table 2** Clinical features and BID/POSTN expression in 135 PTC patients

Characteristics	BID		<i>p</i> value	POSTN		<i>p</i> value
	Low, expres- sion, no. cases	High, expres- sion, no. cases		Low, expres- sion, no. cases	High, expres- sion, no. cases	
Age (years)						
≥ 55	37	34	< 0.001	47	24	0.781
< 55	65	10		48	27	
Gender						
Male	30	9	0.262	22	17	0.185
Female	72	35		73	34	
Tumor size						
≥ 2	35	33	< 0.001	37	31	0.012
< 2	67	11		58	20	
LNM						
Yes	41	31	0.001	26	46	< 0.001
No	61	13		69	5	
ETE						
Yes	4	12	< 0.001	8	8	0.18
No	98	32		87	43	
TNM stage						
I–II	95	11	< 0.001	75	31	0.019
III–IV	7	33		20	20	

LNM, lymph node metastasis; ETE, extrathyroidal extension

extrathyroidal extension ( $p=0.18$ ) were not related to POSTN expression. In addition, the expression of POSTN and BID was further verified in PTC cells (Fig. 8B, C).

## Discussion

THCA is the most common endocrine malignancy and includes papillary thyroid cancer (PTC), follicular thyroid cancer (FTC), poorly differentiated thyroid carcinoma (PDTC), and anaplastic thyroid carcinoma (ATC). Despite improvements in molecular biology techniques, bioinformatics techniques, and a better understanding of THCA, effective treatment of advanced disease remains challenging. Exosomes are actively released by different cell types, thereby conditioning tumor microenvironment; furthermore, exosomes are involved in major functions of tumorigenesis (Feng et al. 2017; Wen et al. 2021). In addition, exosomes are key signals that mediating cell-to-cell communication (Zhang et al. 2016). Accumulating evidence suggests that exosomes could be diagnostic biomarkers, prognostic factors, and therapeutic options for cancer (Ludwig et al. 2017; Peak et al. 2020; Yue et al. 2020). Bioinformatics studies of exosomes have highlighted the key involvement of the prognostic risk assessment model of exosome-related genes in patients with liver

cancer and lung cancer (Li et al. 2021a, b; Zuo et al. 2022). Further analysis revealed that exosome-related genes were associated with the immune microenvironment and prognosis in triple-negative breast cancer, colon adenocarcinoma and gastric cancer (Cui et al. 2022; Lin et al. 2022; Qiu et al. 2021). However, there are few reports on the bioinformatics analysis of exosomes in THCA.

To our knowledge, the present study was the first to establish an exosome risk analysis model based on exosome-related DEGs in THCA patients. The pertinent findings of this study are as follows. First, we obtained 6 exosome-related DEGs (BIRC5, POSTN, TGFBR1, DUSP1, BID, and FGFR2), and the functions and mechanisms of the 6 exosome-related DEGs were analyzed via GO and KEGG enrichment analyses. The protein–protein interaction (PPI), mRNA–miRNA, and mRNA-TF interaction networks were constructed. In addition, the GEO database was used to verify the differential expression of exosome-related DEGs. Moreover, we analyzed the correlation between immune infiltration cell levels and drug sensitivity and the 6 exosome-related DEGs. In addition, our experiments confirmed that the mRNA expression of BID and POSTN was greater in tumor tissue than in normal tissue, whereas the expression levels of DUSP1 and FGFR2 were lower. No statistically significant difference in the expression of TGFBR1 or BIRC5 was observed between these tissues. We further validated the protein expression of BID and POSTN in PTC patients and cell lines.

In our study, 6 exosome-related DEGs were obtained; four (BIRC5, POSTN, TGFBR1, and BID) were upregulated, and two (DUSP1 and FGFR2) were downregulated in THCA. BIRC5 could be used as a diagnostic and prognostic biomarker for tumors, including ovarian cancer and glioma (Xu et al. 2020; Zheng et al. 2022). POSTN is expressed at higher levels in PTC and is associated with invasion and lymph node metastasis (Bai et al. 2009). TGFBR1 is a potent growth inhibitor that can regulate cell growth, and mutations in TGFBR1 are associated with malignant progression and metastasis of tumors (Lin et al. 2017). BID is a proapoptotic Bcl-2 family member that is responsible for apoptotic signaling (Wang et al. 1996) and contributes to multiple cell death paradigms, including oxidative cell death, ferroptosis and mitochondrial damage (Li et al. 2021a, b; Neitemeier et al. 2017; Wang et al. 2021). DUSP1 functions as a tumor suppressor in different tumors (Martinez-Martinez et al. 2021; Zhang et al. 2014), and FGFR2 is a transmembrane tyrosine kinase that mediates the FGF signaling implicated in tumorigenesis (Lei et al. 2021; Turner and Grose 2010). These findings are consistent with the results of our study showing that exosome-related DEGs play significant roles in THCA. Furthermore, the expression status of the 6 genes in our PTC tissues was evaluated by RT–PCR, and the results showed high expression of BID and POSTN. Consistent with our results, POSTN mRNA levels were greater in PTC tissues than in normal tissues and were strongly correlated with tumor metastasis (Bai et al. 2009). BID was upregulated in previous bioinformatics studies (Arora et al. 2021; Wang et al. 2022), and to our knowledge, we found that BID mRNA was overexpressed in PTC cells for the first time. Concurrently, we confirmed that DUSP1 and FGFR2 were downregulated in our PTC tissues compared to their expression in adjacent thyroid tissues, but neither BIRC5 nor TGFBR1 showed statistically significant changes in expression levels.

To gain insight into the biological functions of the exosome-related DEGs, we applied GO/KEGG analyses and revealed that the targets were related to several important signaling pathways, hepatitis B, multiple apoptosis pathways, and the MAPK signaling pathway axis, which are significant cellular signaling pathways in PTC. Importantly, thyroid gland dysfunction has been reported to occur with variant viral infection, and hepatitis B surface antigen (HBsAg) is a risk factor for PTC (Jiang et al. 2022; Zhong et al. 2020). Current and HBsAg-positive PTC patients were more likely to have central lymph node metastasis and bilateral tumors than were HBsAg-negative patients (Zhong et al. 2020).

Furthermore, we employed the 6 genes to construct a PPI network. To extend the interaction, we also incorporated mRNA–miRNA and mRNA–TF interaction networks. In addition, the exosome-related DEGs in THCA and normal tissue samples were compared through TCGA-THCA, GSE3467, and GSE3678. These results support our previous findings that BIRC5, POSTN, TGFBR1, and BID were highly expressed; however, DUSP1 and FGFR2 were expressed at low levels in THCA samples.

THCAs, especially low-risk differentiated thyroid cancer (DTC) tumors, are promising for surgery, thyroid hormone suppression, and radioactive iodine (RAI) therapy; however, the adverse effects of these treatments could be greater than those of the disease itself (Cabanillas et al. 2019). Hence, understanding the mechanisms of immunotherapy and drug sensitivity in THCA patients is highly important (Mandal et al. 2016; Tian et al. 2023a). We performed ssGSEA to quantify the relative abundance of infiltrating immune cells in the TCGA-THCA dataset. Our results demonstrated a close relationship between infiltrating immune cells (central memory CD4 T cells, immature B cells, natural killer cells, regulatory T cells, and T follicular helper cells) and exosome-related DEGs. Screening drugs based on gene expression profiles has been widely applied in modern medicine (Tian et al. 2023b). For drug sensitivity, we profiled the correlation between small molecule drugs and the 6 genes that interacted with the drug molecules to varying degrees. The results showed that DUSP1 interacted with most of the drug molecules in the three databases; however, no drugs were found to interact with TGFBR1 or BID in the GDSC database.

PTC, also known as differentiated thyroid carcinoma, is the most common type THCA in clinical practice, accounting for 70–80% of all thyroid cancer cases, and its incidence rate has gradually increased in recent years. We further focused on novel biomarkers (BID and POSTN) and evaluated protein expression in PTC tissues by IHC. We observed that the protein expression of BID was upregulated in PTC and associated with age, tumor size, lymph node metastasis, extrathyroidal extension, and TNM stage; moreover, our TAM and clinical tissue samples showed that the expression of POSTN was associated with tumor size, lymph node metastasis and TNM stage in patients with PTC. Additionally, the protein expression of these two genes was confirmed in PTC cells.

This study has several limitations. The specific role of exosome-related DEGs, especially BID and POSTN, in PTC should be further studied *in vitro* and *in vivo*. In addition, the mechanisms of exosome-related DEGs in THCA progression

should be explored in further studies, as these findings may lead to new strategies for THCA treatment.

## Conclusions

In conclusion, the exosome-related DEGs were found to be closely related to immune infiltration, drug sensitivity and prognosis in THCA patients. In addition, we experimentally confirmed the expression of novel exosome-related genes in PTC tissues and the relationship between BID/POSTN expression variation and clinicopathologic features in PTC. Our findings may lead to the identification of potential biomarkers and immune candidates for THCA therapeutic strategies.

**Supplementary Information** The online version contains supplementary material available at <https://doi.org/10.1007/s10528-024-10833-2>.

**Acknowledgements** Thanks for all participants who provided samples in this study.

**Author Contributions** Y.W., Q.L., and F.R. cooperated in conceptualization, methodology, writing—original draft preparation and editing. X.Y., H.G., and T.R. collected the clinical cases and biological experiments. T.Z. conducted bioinformatics analysis. P.G. participated in language editing. All authors have read and agreed to the published version of the manuscript.

**Funding** This study was supported by the Middle-aged Scientific and Technological Innovation Foundation of Shenyang City (Grant Number RC210419 to Yiwei Wang); Liaoning Province Science and Technology Research Project (Grant Number LJKMZ20221779 to Yiwei Wang); Shenyang Science and Technology Plan Project “Construction of Shenyang Key Laboratory for Phenomics Research” (Grant Number 21-104-0-26 to Fu Ren).

**Availability of Data and Materials** The data used to support the findings of this study are included within the article.

## Declarations

**Conflict of interest** The authors declare that they have no competing interests.

**Ethical Approval and Consent to Participate** This study was conducted in accordance with the Declaration of Helsinki and approved and agreed to participate by the Ethics Committee of the Affiliated Central Hospital of Shenyang Medical College (approval number: 2023[35]/[36]). This study obtained informed consent from all participants and/or their legal guardians.

**Consent for Publication** All authors agreed to publish this article.

## References

- (1988) 15th meeting of the Japan Endocrine Society, Neuroendocrine Section. *Tsu*, 6 November 1988. Abstract. *Nihon Naibunpi Gakkai Zasshi* 64:901–1000
- Agarwal S, Bychkov A, Jung CK (2021) Emerging biomarkers in thyroid practice and research. *Cancers (Basel)* 14:204
- Allenson K, Castillo J, San Lucas FA, Scelo G, Kim DU, Bernard V et al (2017) High prevalence of mutant KRAS in circulating exosome-derived DNA from early-stage pancreatic cancer patients. *Ann Oncol* 28:741–747

- Arora C, Kaur D, Naorem LD, Raghava GPS (2021) Prognostic biomarkers for predicting papillary thyroid carcinoma patients at high risk using nine genes of apoptotic pathway. *PLoS ONE* 16:e0259534
- Bai Y, Kakudo K, Nakamura M, Ozaki T, Li Y, Liu Z et al (2009) Loss of cellular polarity/cohesiveness in the invasive front of papillary thyroid carcinoma and periostin expression. *Cancer Lett* 281:188–195
- Barretina J, Caponigro G, Stransky N, Venkatesan K, Margolin AA, Kim S et al (2012) The Cancer Cell Line Encyclopedia enables predictive modelling of anticancer drug sensitivity. *Nature* 483:603–607
- Barrett T, Wilhite SE, Ledoux P, Evangelista C, Kim IF, Tomashevsky M et al (2013) NCBI GEO: archive for functional genomics data sets—update. *Nucleic Acids Res* 41:D991–995
- Cabanillas ME, Ryder M, Jimenez C (2019) Targeted therapy for advanced thyroid cancer: kinase inhibitors and beyond. *Endocr Rev* 40:1573–1604
- Cancer Genome Atlas Research N (2014) Integrated genomic characterization of papillary thyroid carcinoma. *Cell* 159:676–690
- Capriglione F, Verrienti A, Celano M, Maggisano V, Sponziello M, Pecce V et al (2022) Analysis of serum microRNA in exosomal vesicles of papillary thyroid cancer. *Endocrine* 75:185–193
- Chen Y, Wang X (2020) miRDB: an online database for prediction of functional microRNA targets. *Nucleic Acids Res* 48:D127–D131
- Colaprico A, Silva TC, Olsen C, Garofano L, Cava C, Garolini D et al (2016) TCGAAbiolinks: an R/Bioconductor package for integrative analysis of TCGA data. *Nucleic Acids Res* 44:e71
- Cui G, Wang C, Liu J, Shon K, Gu R, Chang C et al (2022) Development of an exosome-related and immune microenvironment prognostic signature in colon adenocarcinoma. *Front Genet* 13:995644
- Davis S, Meltzer PS (2007) GEOquery: a bridge between the Gene Expression Omnibus (GEO) and Bioconductor. *Bioinformatics* 23:1846–1847
- Fan CM, Wang JP, Tang YY, Zhao J, He SY, Xiong F et al (2019) circMAN1A2 could serve as a novel serum biomarker for malignant tumors. *Cancer Sci* 110:2180–2188
- Feng Q, Zhang C, Lum D, Druso JE, Blank B, Wilson KF et al (2017) A class of extracellular vesicles from breast cancer cells activates VEGF receptors and tumour angiogenesis. *Nat Commun* 8:14450
- Gan DX, Wang YB, He MY, Chen ZY, Qin XX, Miao ZW et al (2020) Lung cancer cells-controlled Dkk-1 production in brain metastatic cascade drive microglia to acquire a pro-tumorigenic phenotype. *Front Cell Dev Biol* 8:591405
- Ganly I, Makarov V, Deraje S, Dong Y, Reznik E, Seshan V et al (2018) Integrated genomic analysis of Hurthle cell cancer reveals oncogenic drivers, recurrent mitochondrial mutations, and unique chromosomal landscapes. *Cancer Cell* 34(256–270):e255
- Gene Ontology C (2015) Gene Ontology Consortium: going forward. *Nucleic Acids Res* 43:D1049–1056
- He H, Jazdzewski K, Li W, Liyanaratchi S, Nagy R, Volinia S et al (2005) The role of microRNA genes in papillary thyroid carcinoma. *Proc Natl Acad Sci USA* 102:19075–19080
- Ibrahimipac T, Xu B, Landa I, Dogan S, Middha S, Seshan V et al (2017) Genomic alterations in fatal forms of non-anaplastic thyroid cancer: identification of MED12 and RBM10 as novel thyroid cancer genes associated with tumor virulence. *Clin Cancer Res* 23:5970–5980
- Jiang N, Xiang L, He L, Yang G, Zheng J, Wang C et al (2017) Exosomes mediate epithelium–mesenchyme crosstalk in organ development. *ACS Nano* 11:7736–7746
- Jiang H, Li Y, Sheng Q, Dou X (2022) Relationship between Hepatitis B virus infection and platelet production and dysfunction. *Platelets* 33:212–218
- Kanehisa M, Goto S (2000) KEGG: kyoto encyclopedia of genes and genomes. *Nucleic Acids Res* 28:27–30
- Lang FM, Hossain A, Gumin J, Momin EN, Shimizu Y, Ledbetter D et al (2018) Mesenchymal stem cells as natural biofactories for exosomes carrying miR-124a in the treatment of gliomas. *Neuro Oncol* 20:380–390
- Lei JH, Lee MH, Miao K, Huang Z, Yao Z, Zhang A et al (2021) Activation of FGFR2 signaling suppresses BRCA1 and drives triple-negative mammary tumorigenesis that is sensitive to immunotherapy. *Adv Sci (Weinh)* 8:e2100974
- Li JH, Liu S, Zhou H, Qu LH, Yang JH (2014) starBase v2.0: decoding miRNA–ceRNA, miRNA–ncRNA and protein–RNA interaction networks from large-scale CLIP–Seq data. *Nucleic Acids Res* 42:D92–97
- Li J, Gao X, Tian S, Tang M, Liu W (2021a) Exploring exosome data to identify prognostic gene signatures for lung adenocarcinoma. *Future Oncol* 17:4745–4756

- Li K, Xu K, He Y, Lu L, Mao Y, Gao P et al (2021b) Functionalized tumor-targeting nanosheets exhibiting Fe(II) overloading and GSH consumption for ferroptosis activation in liver tumor. *Small* 17:e2102046
- Lin E, Kuo PH, Liu YL, Yang AC, Tsai SJ (2017) Transforming growth factor-beta signaling pathway-associated genes SMAD2 and TGFBR2 are implicated in metabolic syndrome in a Taiwanese population. *Sci Rep* 7:13589
- Lin Y, Huang K, Cai Z, Chen Y, Feng L, Gao Y et al (2022) A novel exosome-relevant molecular classification uncovers distinct immune escape mechanisms and genomic alterations in gastric cancer. *Front Pharmacol* 13:884090
- Ludwig S, Floros T, Theodoraki MN, Hong CS, Jackson EK, Lang S et al (2017) Suppression of lymphocyte functions by plasma exosomes correlates with disease activity in patients with head and neck cancer. *Clin Cancer Res* 23:4843–4854
- Maggisano V, Capriglione F, Verrienti A, Celano M, Gagliardi A, Bulotta S et al (2022) Identification of exosomal microRNAs and their targets in papillary thyroid cancer cells. *Biomedicines* 10:961
- Mandal R, Senbabaoglu Y, Desrichard A, Havel JJ, Dalin MG, Riaz N et al (2016) The head and neck cancer immune landscape and its immunotherapeutic implications. *JCI Insight* 1:e89829
- Martinez-Martinez D, Toledo Lobo MV, Baquero P, Ropero S, Angulo JC, Chiloeches A et al (2021) Downregulation of Snail by DUSP1 impairs cell migration and invasion through the inactivation of JNK and ERK and is useful as a predictive factor in the prognosis of prostate cancer. *Cancers (Basel)* 13:1158
- Neitemeier S, Jelinek A, Laino V, Hoffmann L, Eisenbach I, Eying R et al (2017) BID links ferroptosis to mitochondrial cell death pathways. *Redox Biol* 12:558–570
- Newman AM, Liu CL, Green MR, Gentles AJ, Feng W, Xu Y et al (2015) Robust enumeration of cell subsets from tissue expression profiles. *Nat Methods* 12:453–457
- Nolte-t Hoen E, Cremer T, Gallo RC, Margolis LB (2016) Extracellular vesicles and viruses: Are they close relatives? *Proc Natl Acad Sci USA* 113:9155–9161
- Peak TC, Panigrahi GK, Prahara PP, Su Y, Shi L, Chyr J et al (2020) Syntaxin 6-mediated exosome secretion regulates enzalutamide resistance in prostate cancer. *Mol Carcinog* 59:62–72
- Pozdeyev N, Gay LM, Sokol ES, Hartmaier R, Deaver KE, Davis S et al (2018) Genetic analysis of 779 advanced differentiated and anaplastic thyroid cancers. *Clin Cancer Res* 24:3059–3068
- Qiu P, Guo Q, Yao Q, Chen J, Lin J (2021) Characterization of exosome-related gene risk model to evaluate the tumor immune microenvironment and predict prognosis in triple-negative breast cancer. *Front Immunol* 12:736030
- Reinhold WC, Sunshine M, Liu H, Varma S, Kohn KW, Morris J et al (2012) Cell Miner: a web-based suite of genomic and pharmacologic tools to explore transcript and drug patterns in the NCI-60 cell line set. *Cancer Res* 72:3499–3511
- Ritchie ME, Phipson B, Wu D, Hu Y, Law CW, Shi W et al (2015) limma powers differential expression analyses for RNA-sequencing and microarray studies. *Nucleic Acids Res* 43:e47
- Safran N, Dalah I, Alexander J, Rosen N, Iny Stein T, Shmoish M et al (2010) GeneCards Version 3: the human gene integrator. *Database (Oxford)* 2010:baq020
- Shannon P, Markiel A, Ozier O, Baliga NS, Wang JT, Ramage D et al (2003) Cytoscape: a software environment for integrated models of biomolecular interaction networks. *Genome Res* 13:2498–2504
- Tian S, Li Y, Xu J, Zhang L, Zhang J, Lu J et al (2023a) COIMMR: a computational framework to reveal the contribution of herbal ingredients against human cancer via immune microenvironment and metabolic reprogramming. *Brief Bioinform* 24:bbad346
- Tian S, Zhang J, Yuan S, Wang Q, Lv C, Wang J et al (2023b) Exploring pharmacological active ingredients of traditional Chinese medicine by pharmacotranscriptomic map in ITCM. *Brief Bioinform* 24:bbad027
- Tomczak K, Czerwinska P, Wiznerowicz M (2015) The Cancer Genome Atlas (TCGA): an immeasurable source of knowledge. *Contemp Oncol (Pozn)* 19:A68–77
- Turner N, Grose R (2010) Fibroblast growth factor signalling: from development to cancer. *Nat Rev Cancer* 10:116–129
- Villarroya-Beltri C, Baixauli F, Mittelbrunn M, Fernandez-Delgado I, Torralba D, Moreno-Gonzalo O et al (2016) ISGylation controls exosome secretion by promoting lysosomal degradation of MVB proteins. *Nat Commun* 7:13588
- Wang K, Yin XM, Chao DT, Millman CL, Korsmeyer SJ (1996) BID: a novel BH3 domain-only death agonist. *Genes Dev* 10:2859–2869

- Wang X, Sun Z, Tian W, Piao C, Xie X, Zang J et al (2020) S100A12 is a promising biomarker in papillary thyroid cancer. *Sci Rep* 10:1724
- Wang ZX, Ma J, Li XY, Wu Y, Shi H, Chen Y et al (2021) Quercetin induces p53-independent cancer cell death through lysosome activation by the transcription factor EB and reactive oxygen species-dependent ferroptosis. *Br J Pharmacol* 178:1133–1148
- Wang Y, Yang J, Chen S, Wang W, Teng L (2022) Identification and validation of a prognostic signature for thyroid cancer based on ferroptosis-related genes. *Genes (Basel)* 13:997
- Wen D, Liu WL, Lu ZW, Cao YM, Ji QH, Wei WJ (2021) SNHG9, a papillary thyroid cancer cell exosome-enriched lncRNA, inhibits cell autophagy and promotes cell apoptosis of normal thyroid epithelial cell Nthy-ori-3 through YBOX3/P21 pathway. *Front Oncol* 11:647034
- Wu F, Li F, Lin X, Xu F, Cui RR, Zhong JY et al (2019) Exosomes increased angiogenesis in papillary thyroid cancer microenvironment. *Endocr Relat Cancer* 26:525–538
- Xie X, Nie H, Zhou Y, Lian S, Mei H, Lu Y et al (2019) Eliminating blood oncogenic exosomes into the small intestine with aptamer-functionalized nanoparticles. *Nat Commun* 10:5476
- Xin Y, Meng K, Guo H, Chen B, Zheng C, Shou X et al (2022) Exosomal hsa-miR-129-2 and hsa-miR-889 from a 6-microRNA signature might be a potential biomarker for predicting the prognosis of papillary thyroid carcinoma. *Comb Chem High Throughput Screen* 25:819–830
- Xu Y, Li R, Li X, Dong N, Wu D, Hou L et al (2020) An autophagy-related gene signature associated with clinical prognosis and immune microenvironment in gliomas. *Front Oncol* 10:571189
- Yang W, Soares J, Greninger P, Edelman EJ, Lightfoot H, Forbes S et al (2013) Genomics of drug sensitivity in cancer (GDSC): a resource for therapeutic biomarker discovery in cancer cells. *Nucleic Acids Res* 41:D955–961
- Yoo SK, Song YS, Lee EK, Hwang J, Kim HH, Jung G et al (2019) Integrative analysis of genomic and transcriptomic characteristics associated with progression of aggressive thyroid cancer. *Nat Commun* 10:2764
- Yu G, Wang LG, Han Y, He QY (2012) clusterProfiler: an R package for comparing biological themes among gene clusters. *OMICS* 16:284–287
- Yue Y, Wang C, Benedict C, Huang G, Truongcao M, Roy R et al (2020) Interleukin-10 deficiency alters endothelial progenitor cell-derived exosome reparative effect on myocardial repair via integrin-linked kinase enrichment. *Circ Res* 126:315–329
- Zhang X, Hyer JM, Yu H, D'Silva NJ, Kirkwood KL (2014) DUSP1 phosphatase regulates the proinflammatory milieu in head and neck squamous cell carcinoma. *Cancer Res* 74:7191–7197
- Zhang H, Xiang M, Meng D, Sun N, Chen S (2016) Inhibition of myocardial ischemia/reperfusion injury by exosomes secreted from mesenchymal stem cells. *Stem Cells Int* 2016:4328362
- Zhang Q, Liu W, Zhang HM, Xie GY, Miao YR, Xia M et al (2020) hTFtarget: a comprehensive database for regulations of human transcription factors and their targets. *Genom Proteom Bioinform* 18:120–128
- Zheng Q, Ye H, Zhong H, Wang M (2022) Identification of biomarkers for ovarian cancer diagnosis and prognosis by bioinformatics analysis and q-PCR Validation. *Ann Clin Lab Sci* 52:967–975
- Zhong Z, Yuan J, Chen X, Chen Z, Du J, Chen Z et al (2020) The clinicopathological features of papillary thyroid carcinoma patients with positive hepatitis B surface antigen. *Oncol Res Treat* 43:27–33
- Zhou KR, Liu S, Sun WJ, Zheng LL, Zhou H, Yang JH et al (2017) ChIPBase v2.0: decoding transcriptional regulatory networks of non-coding RNAs and protein-coding genes from ChIP-seq data. *Nucleic Acids Res* 45:D43–D50
- Zou X, Gao F, Wang ZY, Zhang H, Liu QX, Jiang L et al (2020) A three-microRNA panel in serum as novel biomarker for papillary thyroid carcinoma diagnosis. *Chin Med J (Engl)* 133:2543–2551
- Zuo B, Kuai J, Long J, Bian J, Yang X, Yang X et al (2022) Differentially expressed liver exosome-related genes as candidate prognostic biomarkers for hepatocellular carcinoma. *Ann Transl Med* 10:817

**Publisher's Note** Springer Nature remains neutral with regard to jurisdictional claims in published maps and institutional affiliations.

Springer Nature or its licensor (e.g. a society or other partner) holds exclusive rights to this article under a publishing agreement with the author(s) or other rightsholder(s); author self-archiving of the accepted manuscript version of this article is solely governed by the terms of such publishing agreement and applicable law.

## Authors and Affiliations

Yiwei Wang<sup>1,2,7</sup> · Qiang Li<sup>3</sup> · Xinrui Yang<sup>2</sup> · Hanyu Guo<sup>1</sup> · Tian Ren<sup>4</sup> ·  
Tianchi Zhang<sup>5</sup> · Pantea Ghadakpour<sup>6</sup> · Fu Ren<sup>1,7</sup>

✉ Fu Ren  
rf@symc.edu.cn

- <sup>1</sup> Department of Anatomy, College of Basic Medical Sciences of Shenyang Medical College, Shenyang, Liaoning, People's Republic of China
- <sup>2</sup> Molecular Morphology Laboratory, College of Basic Medical Sciences, Liaoning, Shenyang Medical College, Shenyang, People's Republic of China
- <sup>3</sup> Department of Orthopedics, Liaoning, Fuxin Central Hospital, Fuxin, People's Republic of China
- <sup>4</sup> Emergency Medical Center, Liaoning, Affiliated Central Hospital of Shenyang Medical College, Shenyang, People's Republic of China
- <sup>5</sup> Department of Computer and Information Technology, University of Pennsylvania, Philadelphia, PA, United States
- <sup>6</sup> Department of Biology, George Mason University, Fairfax, VA, USA
- <sup>7</sup> Key Laboratory of Human Ethnic Specificity and Phenomics of Critical Illness in Liaoning Province, Shenyang Medical College, Shenyang, Liaoning, People's Republic of China